2. Discrete Population Models for a Single Species

2.1 Introduction: Simple Models

Differential equation models, whether ordinary, delay, partial or stochastic, imply a continuous overlap of generations. Many species have no overlap whatsoever between successive generations and so population growth is in discrete steps. For primitive organisms these can be quite short in which case a continuous (in time) model may be a reasonable approximation. However, depending on the species the step lengths can vary widely. A year is common. With fruit fly emergence from pupae it is a day, for cells it can be a number of hours while for bacteria and viruses it can be considerably less. In the models we discuss in this chapter and later in Chapter 5 we have scaled the time-step to be 1. Models must thus relate the population at time $t+1$, denoted by N_{t+1}, in terms of the population N_t at time t. This leads us to study difference equations, or discrete models, of the form

$$N_{t+1} = N_t F(N_t) = f(N_t), \tag{2.1}$$

where $f(N_t)$ is in general a nonlinear function of N_t. The first form is often used to emphasise the existence of a zero steady state. Such equations are usually impossible to solve analytically but again we can extract a considerable amount of information about the population dynamics without an analytical solution. The mathematics of difference equations is now being studied in depth and applied in diverse fields: it is a fascinating subject having given rise to some totally unexpected phenomena some of which we discuss later. Difference equation models are also proving of use in a surprisingly wide spectrum of biomedical areas such as cancer growth (see, for example, the article by Cross and Cotton 1994), aging (see, for example, the article by Lipsitz and Goldberger 1992), cell proliferation (see, for example, the article by Hall and Levinson 1990) and genetics (see, for example, the chapter on inheritance in the book by Hoppensteadtand Peskin 1992 and the book by Roughgarden 1996.) It has recently been shown to be of astonishing use in dynamic modelling of marital interaction and divorce prediction; we discuss this application in Chapter 5. The largest use to date is probably in ecology; the book by Hassell (1978) gives numerous examples, see also the more recent excellent book by Kot (2001).

From a practical point of view, if we know the form of $f(N_t)$ it is a straightforward matter to evaluate N_{t+1} and subsequent generations by simply using (2.1) recursively.

Of course, whatever the form of $f(N_t)$, we are only interested in nonnegative populations.

The skill in modelling a specific population's growth dynamics lies in determining the appropriate form of $f(N_t)$ to reflect known observations or facts about the species in question. To do this with any confidence we must understand the major effects on the solutions of changes in the form of $f(N_t)$ and its parameters, and also what solutions of (2.1) look like for a few specimen examples of practical interest. The mathematical problem is a mapping one, namely, that of finding the orbits, or trajectories, of nonlinear maps given a starting value $N_0 > 0$. It should be noted here that there is no simple connection between difference equation models and what might appear to be the continuous differential equation analogue, even though a finite difference approximation results in a discrete equation. This becomes clear below.

Suppose the function $F(N_t) = r > 0$; that is, the population one step later is simply proportional to the current population. Then from (2.1),

$$N_{t+1} = rN_t \quad \Rightarrow \quad N_t = r^t N_0. \tag{2.2}$$

So the population grows or decays geometrically according to whether $r > 1$ or $r < 1$ respectively; here r is the net reproductive rate. This particularly simple model is not very realistic for most populations nor for long times but, even so, it has been used with some justification for the early stages of growth of certain bacteria. It is the discrete version of Malthus' model in Chapter 1. A slight modification to bring in crowding effects could be

$$N_{t+1} = rN_S, \quad N_S = N_t^{1-b}, \quad b \text{ constant},$$

where N_S is the population that survives to breed. There must be restrictions on b of course, so that $N_S \leq N_t$ otherwise those surviving to breed would be more than the population of which they form a part.

Fibonacci Sequence

Leonardo of Pisa, who was only given the nickname Fibonacci in the 18th century, in his arithmetic book of 1202 set a modelling exercise involving an hypothetical growing rabbit population. It consists of starting at the beginning of the breeding season with a pair of immature rabbits, male and female, which after one reproductive season produce two pairs of male and female immature rabbits after which the parents then stop reproducing. Their offspring pairs then do exactly the same and so on. The question is to determine the number of pairs of rabbits at each reproductive period. If we denote the number of pairs of (male and female) rabbits by N_t then normalising the reproductive period to 1 we have at the tth reproductive stage

$$N_{t+1} = N_t + N_{t-1}, \quad t = 2, 3, \ldots . \tag{2.3}$$

This gives, with $N_0 = 1$, what is known as the Fibonacci sequence, namely

$$1, 1, 2, 3, 5, 8, 13, \ldots .$$

Each term in the sequence is simply the sum of the previous two. Equation (2.3) is a linear difference equation which we can solve by looking for solutions in the form

$$N_t \propto \lambda^t$$

which on substituting into (2.3) gives the equation for the λ as solutions of

$$\lambda^2 - \lambda - 1 \quad \Rightarrow \quad \lambda_{1,2} = \frac{1}{2}\left(1 \pm \sqrt{5}\right).$$

So, with $N_0 = 1$, $N_1 = 1$ the solution of (2.3) is

$$\begin{aligned} N_t &= \frac{1}{2}\left(1 + \frac{1}{\sqrt{5}}\right)\lambda_1^t + \frac{1}{2}\left(1 - \frac{1}{\sqrt{5}}\right)\lambda_2^t \\ \lambda_1 &= \frac{1}{2}\left(1 + \sqrt{5}\right), \quad \lambda_2 = \frac{1}{2}\left(1 - \sqrt{5}\right). \end{aligned} \tag{2.4}$$

For large t, since $\lambda_1 > \lambda_2$,

$$N_t \approx \frac{1}{2}\left(1 + \frac{1}{\sqrt{5}}\right)\lambda_1^t.$$

Equation (2.3) is a renewal equation. We can intuitively see age structure in this model by considering age to reproduction and that after it there is no reproduction. This approach gives rise to renewal matrices and Leslie matrices which include age structure (see, for example, the book edited by Caswell 1989).

If we take the ratio of successive Fibonacci numbers we have, for t large, $N_t/N_{t+1} \approx (\sqrt{5} - 1)/2$. This is the so-called golden mean or golden number. In classical paintings, for example, it is the number to strive for in the ratio of say, sky to land in a landscape.

This sequence and the limiting number above occur in a surprising number of places. Pine cones, sunflower heads, daisy florets, angles between successive branching in many plants and many more. On a sunflower head, it is possible to see sets of intertwined spirals emanating from the centre (you can see them on pine cones starting at the base). It turns out that the number of spirals varies but are always a number in the Fibonacci sequence.

Figure 2.1 illustrates two examples of these naturally occurring intertwined logarithmic spirals. For example, in Figure 2.1(b) each scale belongs to both a clockwise and anticlockwise spiral: a careful counting gives 8 clockwise spirals and 13 anticlockwise ones, which are consecutive numbers in the Fibonacci series. On the daisy head there are 21 clockwise and 34 anticlockwise spirals, again consecutive numbers in the Fibonacci series.

In the case of branching in phyllotaxis, if you project the branching of many plants and trees onto the plane the angle between successive branches is essentially constant, close to 137.5°. To relate this to the Fibonacci series, if we multiply 360° by the limiting number of the ratio of Fibonacci numbers above, $(\sqrt{5} - 1)/2$, we get 222.5°. Since this is more than 180° we should subtract 222.5° from 360° which gives 137.5°, which is known as the *Fibonacci angle*.

(**a**)

(**b**)

Figure 2.1. Examples of sets of intertwining spirals which occur on (**a**) the floret of a daisy, and (**b**) the pattern of scales on a pine cone. Each element is part of a clockwise and anticlockwise spiral. (Photographs by Dr. Scott Camazine and reproduced with permission)

There have been several attempts at modelling the patterning process in plant morphology to generate the Fibonacci angle between successive branches and the Fibonacci sequence for the number of spirals on sunflower heads, pine cones, and so on but to date the problem is still unsolved. The attempts range from manipulating a reaction diffusion mechanism (for example, Thornley 1976) to looking at algebraic relations between permutations of the first n natural numbers with each number corresponding to the initiation order of a given leaf (Kunz and Rothen 1992) to experiments involving magnetic droplets in a magnetic field (Douady and Couder 1992). Later in the book we discuss in considerable detail various possible mechanisms for generating spatial patterns, including reaction diffusion systems. I firmly believe that the process here is mechanistic

and *not* genetic. The work of Douady and Couder (1992, 1993a, 1993b), although of a physical rather than a biological nature, lends support to this belief.

The work of Douady and Couder (1992) is clever and particularly interesting and illuminating even though it is a physical as opposed to a biological process involved. They considered the sequential appearance of the primordia in branching phyllotaxis to form at the growing apex and at equal time intervals to move out onto a circle around the growing tip. They considered these primordia to repel each other as they move out, consequently maximising the distance between them. In this way they self-organise themselves highly efficiently in a regular spatial pattern. If this is the case, they argued, then an experiment which mimics this scenario should give a distribution of elements, the angle between which should be the Fibonacci angle. They took a circular dish of 8 cm diameter, filled it with silicone oil and put it in a vertical magnetic field with the field increasing towards the dish perimeter. Then, at equal intervals, they dropped small amounts of a ferromagnetic fluid onto the centre of the dish onto a small truncated cone (to simulate the plant apex). The drops were then polarised by the magnetic field. Because of the polarisation the drops formed small magnetic dipoles which repelled each other and, because of the gradient in the magnetic field, moved outwards towards the perimeter and ended up being regularly distributed. Because of the interaction with the previous drops, new drops fell from the cone in the direction of minimum energy. To prevent accumulation of drops at the periphery, they ultimately fell into a ditch there. The time between the drops of magnetic fluid affected the spirals generated and the final angle between the drops when they reached the perimeter: in a surprising number of runs the angle was essentially the Fibonacci angle and the number of spirals a number in the Fibonacci series. They then confirmed the results with computer simulations.

Generally, because of crowding and self-regulation, we expect $f(N_t)$ in (2.1) to have some maximum, at N_m say, as a function of N_t with f decreasing for $N_t > N_m$; Figure 2.2 illustrates a typical form. A variety of $f(N_t)$ has been used in practical situations such as those described above: see, for example, the book by Kot (2001) for some specific practical forms in ecology. One such model, sometimes referred to as the

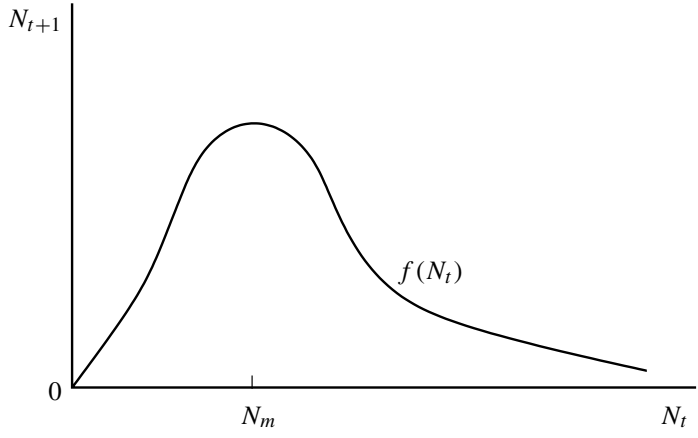

Figure 2.2. Typical growth form in the model $N_{t+1} = f(N_t)$.

Verhulst process, is

$$N_{t+1} = rN_t\left(1 - \frac{N_t}{K}\right), \quad r > 0, \quad K > 0, \tag{2.5}$$

which might appear to be a kind of discrete analogue of the continuous logistic growth model but is not all: the steady state is *not* $N = K$. As we shall show, however, the solutions and their dependence on the parameter r are very different. An obvious drawback of this specific model is that if $N_t > K$ then $N_{t+1} < 0$. A more appropriate way of deriving it (see also the legend in Figure 2.11) from the continuous Verhulst equation is to replace the derivative dN/dt with a difference form with time step 1 to obtain

$$N(t+1) - N(t) = rN(t)\left[1 - \frac{N(t)}{K}\right] \Rightarrow N(t+1) = \left[1 + r - \frac{r}{K}N(t)\right]. \tag{2.6}$$

Now rescaling with $N(t) = ((1+r)/r)Kx(t)$ and setting $1 + r = r'$ the last equation becomes the same form as (2.2), namely,

$$x(t+1) = r'x(t)[1 - x(t)]. \tag{2.7}$$

A more realistic model should be such that for large N_t there should be a reduction in the growth rate but N_{t+1} should remain nonnegative; the qualitative form for $f(N_t)$ in Figure 2.2 is an example. One such frequently used model, known as the Ricker curve, after Ricker (1954), is

$$N_{t+1} = N_t \exp\left[r\left(1 - \frac{N_t}{K}\right)\right], \quad r > 0, \quad K > 0 \tag{2.8}$$

which we can think of as a modification of (2.2) where there is a mortality factor $\exp(-rN_t/K)$ which is more severe the larger N_t. Here $N_t > 0$ for all t if $N_0 > 0$.

Since t increases by discrete steps there is, in a sense, an inherent *delay* in the population to register change. Thus there is a certain heuristic basis for relating these difference equations to delay differential equations discussed in Chapter 1, which, depending on the length of the delay, could have oscillatory solutions. Since we scaled the time-step to be 1 in the general form (2.1) we should expect the other parameters to be the controlling factors as to whether or not solutions are periodic. With (2.5) and (2.8) the determining parameter is r, since K can be scaled out by writing N_t for N_t/K.

2.2 Cobwebbing: A Graphical Procedure of Solution

We can elicit a considerable amount of information about the population growth behaviour by simple graphical means. Consider (2.1) with f as in Figure 2.2. The steady states are solutions N^* of

$$N^* = f(N^*) = N^*F(N^*) \quad \Rightarrow \quad N^* = 0 \quad \text{or} \quad F(N^*) = 1. \tag{2.9}$$

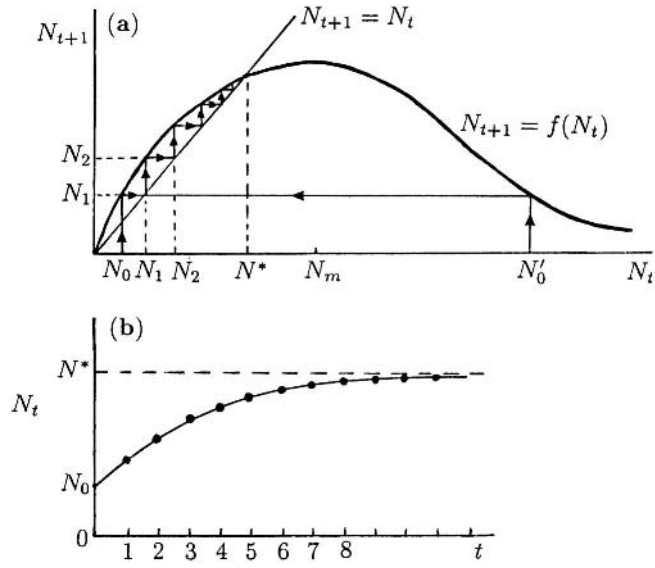

Figure 2.3. (**a**) Graphical determination of the steady state and demonstration of how N_t approaches it. (**b**) Time evolution of the population growth using (**a**). We use a continuous curve joining up the populations at different time-steps for visual clarity; strictly the population changes abruptly at each time-step.

Generally, we use only the first form in (2.9); the second is mainly used to emphasise the fact that $N^* = 0$ is always a steady state. Graphically the steady states are intersections of the curve $N_{t+1} = f(N_t)$ and the straight line $N_{t+1} = N_t$ as shown in Figure 2.3(a) for a case where the maximum of the curve $N_{t+1} = f(N_t)$, at N_m say, has $N_m > N^*$. The dynamic evolution of the solution N_t of (2.1) can be obtained graphically as follows. Suppose we start at N_0 in Figure 2.3(a). Then N_1 is given by simply moving along the N_{t+1} axis until we intersect with the curve $N_{t+1} = f(N_t)$, which gives $N_1 = f(N_0)$. The line $N_{t+1} = N_t$ is now used to start again with N_1 in place of N_0. We then get N_2 by proceeding as before and then N_3, N_4 and so on: the arrows show the path sequence. The path is simply a series of reflections in the line $N_{t+1} = N_t$. We see that $N_t \to N^*$ as $t \to \infty$ and it does so monotonically as illustrated in Figure 2.3(b). If we started at $N_0' > N^*$ in Figure 2.3(a), again $N_t \to N^*$ and monotonically after the first step. If we start close enough to the steady state N^* the approach to it is monotonic as long as the curve $N_{t+1} = f(N_t)$ crosses $N_{t+1} = N_t$ appropriately; here that means

$$0 < \left[\frac{df(N_t)}{dN_t}\right]_{N_t=N^*} = f'(N^*) < 1. \tag{2.10}$$

The value $f'(N^*)$, where the prime denotes the derivative with respect to N_t, is an important parameter as we shall show; it is the *eigenvalue* of the system at the steady state N^*. Since any small perturbation about N^* simply decays to zero, N^* is a linearly stable equilibrium state.

Suppose now $f(N_t)$ is such that the equilibrium $N^* > N_m$ as in Figure 2.4. The dynamic behaviour of the population depends critically on the geometry of the intersection of the curves at N^* as seen from the inset enlargements in Figures 2.4(a), (b) and (c): these respectively have $-1 < f'(N^*) < 0$, $f'(N^*) = -1$ and $f'(N^*) < -1$. The solution N_t is oscillatory in the vicinity of N^*. If the oscillations decrease in amplitude and $N_t \to N^*$ then N^* is stable as in Figure 2.4(a), while it is unstable if the oscillations grow as in Figure 2.4(c). The case Figure 2.4(b) exhibits oscillations which are periodic and suggest that periodic solutions to the equation $N_{t+1} = f(N_t)$ are possible. The steady state is strictly unstable if a small perturbation from N^* does not tend to zero. The population's dynamic behaviour for each of the three cases in Figure 2.4 is illustrated in Figure 2.5.

The parameter $\lambda = f'(N^*)$, the eigenvalue of the equilibrium N^* of $N_{t+1} = f(N_t)$, is crucial in determining the local behaviour about the steady state. The cases in which the behaviour is clear and decisive are when $0 < \lambda < 1$ as in Figure 2.3(a) and $-1 < \lambda < 0$ and $\lambda < -1$ as in Figures 2.4(b) and (c) respectively. The equilibrium is stable if $-1 < \lambda < 1$ and is said to be an *attracting equilibrium.* The critical *bifurcation* values $\lambda = \pm 1$ are where the solution N_t changes its behavioural character. The case $\lambda = 1$ is where the curve $N_{t+1} = f(N_t)$ is tangent to $N_{t+1} = N_t$ at the steady state since $f'(N^*) = 1$, and is called a *tangent bifurcation* for obvious reasons. The case

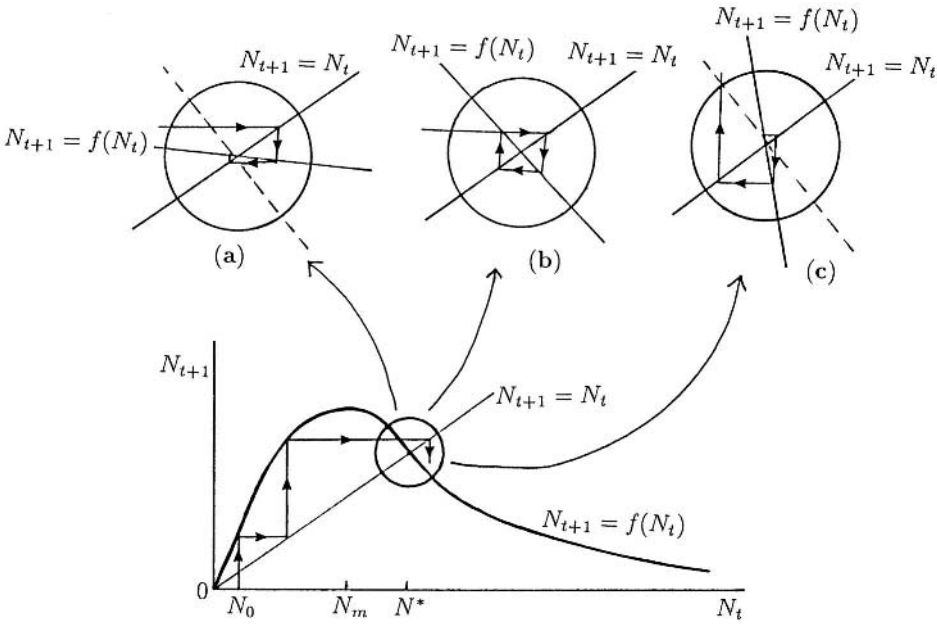

Figure 2.4. Local behaviour of N_t near a steady state where $f'(N^*) < 0$. The enlargements show the cases where (**a**) $-1 < f'(N^*) < 0$, N^* is stable with decreasing oscillations for any small perturbation from the steady state. (**b**) $f'(N^*) = -1$, N^* is neutrally stable. (**c**) $f'(N^*) < -1$, N^* is unstable with growing oscillations.

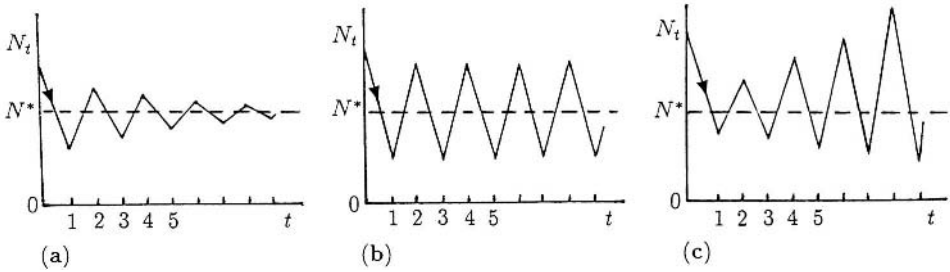

Figure 2.5. Local behaviour of small perturbations about the equilibrium population N^* with (**a**), (**b**), and (**c**) corresponding to the situations illustrated in Figures 2.3 (a), (b) and (c) respectively: (**a**) is the stable case and (**c**) the unstable case.

$\lambda = -1$ for reasons that will become clear used to be called a *pitchfork* bifurcation but is now referred to as a *period-doubling bifurcation*.

The reason for the colourful description 'cobwebbing' for this graphical procedure is obvious from Figures 2.3, 2.4 and 2.6. It is an exceedingly useful procedure for suggesting the dynamic behaviour of the population N_t for single equations of the type (2.1). Although we have mainly concentrated on the local behaviour near an equilibrium it also gives the quantitative global behaviour. If the steady state is unstable, it can presage the peculiar behaviour that solutions of such equations can exhibit. As an example suppose $\lambda = f'(N^*) < -1$; that is, the local behaviour near the unstable N^* is as in Figure 2.4(c). If we now cobweb such a case we have a situation such as shown in Figure 2.6. The solution trajectory cannot tend to N^*. On the other hand, the population must be bounded by $N_{\max}$ in Figure 2.6(a) since there is no way we can generate a larger N_t although we could start with one. Thus the solution is globally bounded but does not tend to a steady state. In fact it seems to wander about in a seemingly random

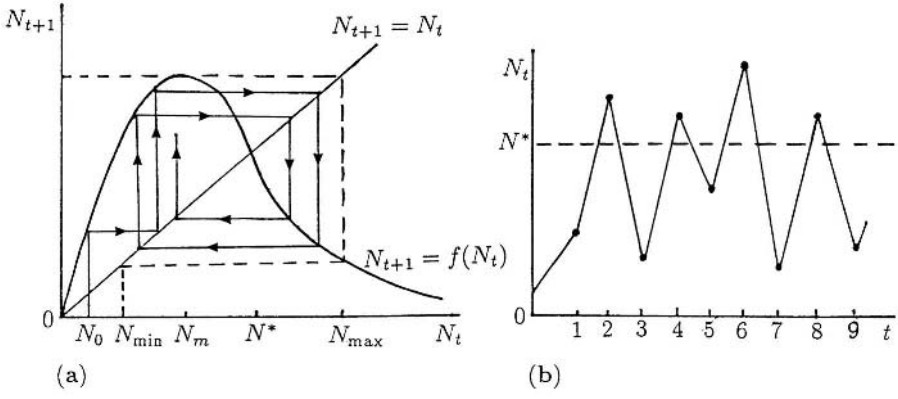

Figure 2.6. (**a**) Cobweb for $N_{t+1} = f(N_t)$ where the eigenvalue $\lambda = f'(N^*) < -1$. (**b**) The corresponding population behaviour as a function of time.

way if we look at it as a function of time in Figure 2.6(b). Solutions which do this are called *chaotic*.

With the different kinds of solutions of models like (2.1), as indicated by the cobweb procedure and the sensitivity hinted at by the special critical values of the eigenvalue λ, we must now investigate such equations analytically. The results suggested by the graphical approach can be very helpful in the analysis.

2.3 Discrete Logistic-Type Model: Chaos

As a concrete example consider the nonlinear logistic-type model

$$u_{t+1} = ru_t(1 - u_t), \quad r > 0, \tag{2.11}$$

where we assume $0 < u_0 < 1$ and we are interested in solutions $u_t \geq 0$. From the relation to the continuous differential equation logistic model the 'r' here is strictly '$1 + r$'. The steady states and corresponding eigenvalues λ are

$$\begin{aligned} u^* &= 0, \quad \lambda = f'(0) = r, \\ u^* &= \frac{r-1}{r}, \quad \lambda = f'(u^*) = 2 - r. \end{aligned} \tag{2.12}$$

As r increases from zero but with $0 < r < 1$ the only realistic, that is, nonnegative, equilibrium is $u^* = 0$ which is stable since $0 < \lambda < 1$. It is also clear from a cobwebbing of (2.11) with $0 < r < 1$ or analytically from equation (2.11) on noting that $u_1 < u_0 < 1$ and $u_{t+1} < u_t$ for all t, which implies that $u_t \to 0$ as $t \to \infty$.

The first bifurcation comes when $r = 1$ since $u^* = 0$ becomes unstable since its eigenvalue $\lambda > 1$ for $r > 1$, while the positive steady state $u^* = (r - 1)/r > 0$, for which $-1 < \lambda < 1$ for $1 < r < 3$, is stable for this range of r. The second bifurcation is at $r = 3$ where $\lambda = -1$. Here $f'(u^*) = -1$, and so, locally near u^*, we have the situation in Figure 2.4(b) which exhibits a periodic solution.

To see what is happening when r passes through the bifurcation value $r = 3$, let us first introduce the following notation for the iterative procedure,

$$\begin{cases} u_1 = f(u_0) \\ u_2 = f(f(u_0)) = f^2(u_0) \\ \quad \vdots \\ u_t = f^t(u_0) \end{cases}. \tag{2.13}$$

With the example (2.11) the first iteration is simply the equation (2.11) while the second iterate is

$$u_{t+2} = f^2(u_t) = r[ru_t(1 - u_t)][1 - ru_t(1 - u_t)]. \tag{2.14}$$

Figure 2.7(a) illustrates the effect on the first iteration as r varies; the eigenvalue $\lambda = f'(u^*)$ decreases as r increases and $\lambda = -1$ when $r = 3$. We now look at the

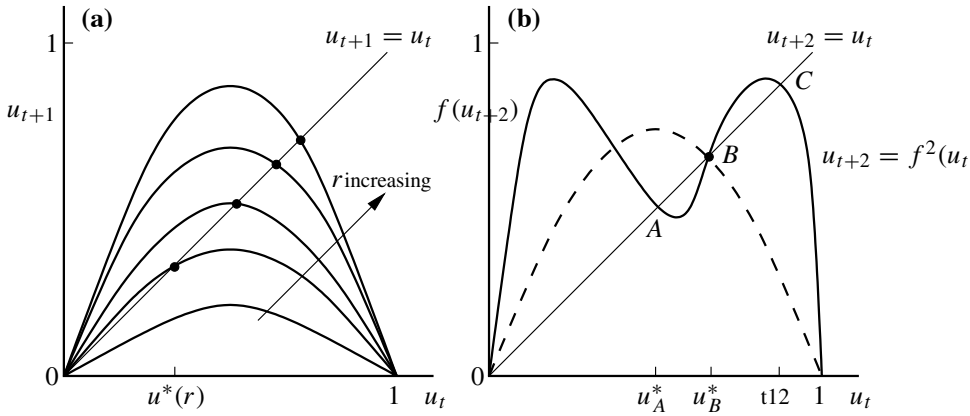

Figure 2.7. (**a**) First iteration as a function of r for $u_{t+1} = ru_t(1-u_t)$: $u^* = (r-1)/r$, $\lambda = f'(u^*) = 2-r$. (**b**) Sketch of the second iteration $u_{t+2} = f^2(u_t)$ as a function of u_t for $r = 3+\varepsilon$ where $0 < \varepsilon \ll 1$. The dashed line reproduces the first iteration curve of u_{t+1} as a function of u_t; it passes through B, the unstable steady state. The curve is symmetric about $u_t = 1/2$.

second iteration (2.14) and ask if it has any equilibria, that is, where $u_{t+2} = u_t = u_2^*$. A little algebra shows that u_2^* satisfies

$$u_2^*[ru_2^* - (r-1)][r^2 u_2^{*2} - r(r+1)u_2^* + (r+1)] = 0 \tag{2.15}$$

which has solutions

$$\begin{aligned} u_2^* &= 0 \quad \text{or} \quad u_2^* = \frac{r-1}{r} > 0 \quad \text{if} \quad r > 1, \\ u_2^* &= \frac{(r+1) \pm [(r+1)(r-3)]^{1/2}}{2r} > 0 \quad \text{if} \quad r > 3. \end{aligned} \tag{2.16}$$

We thus see that there are 2 more real steady states of $u_{t+2} = f^2(u_t)$ with $f(u_t)$ from (2.11) if $r > 3$. This corresponds to the situation in Figure 2.7(b) where A, B and C are the positive equilibria u_2^*, with B equal to $(r-1)/r$, lying between the two new solutions for u_2^* in (2.16) which appear when $r > 3$.

We can think of (2.14) as a first iteration in a model where the iterative time step is 2. The eigenvalues λ of the equilibria can be calculated at the points A, B and C. Clearly $\lambda_B = f'(u_B^*) > 1$ from Figure 2.7(b) where u_B^* denotes u_2^* at B and similarly for A and C. For r just greater than 3, $-1 < \lambda_A < 1$ and $-1 < \lambda_C < 1$ as can be seen visually or, from (2.14), by evaluating $\partial f^2(u_t)/\partial u_t$ at u_A^* and u_C^* given by the last two solutions in (2.16). Thus the steady states, u_A^* and u_C^*, of the second iteration (2.14) are stable. What this means is that there is a stable equilibrium of the second iteration (2.14) and this means that there exists a stable *periodic solution* of period 2 of equation (2.11). In other words if we start at A, for example, we come back to it after 2 iterations, that is $u_{A+2}^* = f^2(u_A^*)$ but $u_{A+1}^* = f(u_A^*) \neq u_A^*$. In fact $u_{A+1}^* = u_C^*$ and $u_{C+1}^* = u_A^*$.

As r continues to increase, the eigenvalues λ at A and C in Figure 2.7(b) pass through $\lambda = -1$ and so these 2-period solutions become unstable. At this stage we look at the 4th iterate and we find, as might now be expected, that u_{t+4} as a function of u_t will have four humps as compared with two in Figure 2.7(b) and a 4-cycle periodic solution appears. Thus as r passes through a series of bifurcation values the character of the solution u_t passes through a series of bifurcations, here in period doublingof the periodic solutions. The bifurcation situation is illustrated in Figure 2.8(a). These bifurcations when $\lambda = -1$ were originally called *pitchfork bifurcations* for obvious reasons from the picture they generate in Figure 2.8(a). However, since it is only a pitchfork from the point of view of two-cycles it is now called a period-doubling bifurcation. For example, if $3 < r < r_4$, where r_4 is the bifurcation value to a 4-period solution, then the periodic solution is between the two u^* in Figure 2.8(a) which are the intersections of the vertical line through the r value and the curve of equilibrium states. Figure 2.8(b) is an example of a 4-cycle periodic solution, that is, $r_4 < r < r_8$ with the actual u_t values again given by the 4 intersections of the curve of equilibrium states with the vertical line through that value of r.

As r increases through successive bifurcations, every even p-periodic solution branches into a $2p$-periodic solution and this happens when r is such that the eigenvalue of the p-periodic solution passes through -1. The distance between bifurcations in r-space gets smaller and smaller: this is heuristically plausible since higher order iterates imply more humps (compare with Figure 2.7(b)) all of which are fitted into the same interval $(0, 1)$. There is thus a hierarchy of solutions of period 2^n for every n, and associated with each, is a parameter interval in which it is stable. There is a limiting value r_c at which instability sets in for all periodic solutions of period 2^n. For $r > r_c$ all the original 2^n-cycles are unstable. The behaviour is quite complex. For $r > r_c$ odd cycles begin to appear and a simple 3-cycle eventually appears when $r \approx 3.828$ and locally attracting cycles with periods $k, 2k, 4k, \ldots$ appear but where now k is *odd*. Another stable 4-cycle, for example, shows up when $r \approx 3.96$.

This critical parameter value r_c in our model (2.11) is when odd period solutions are just possible. When the third iterate has 3 steady states which are tangent to the line

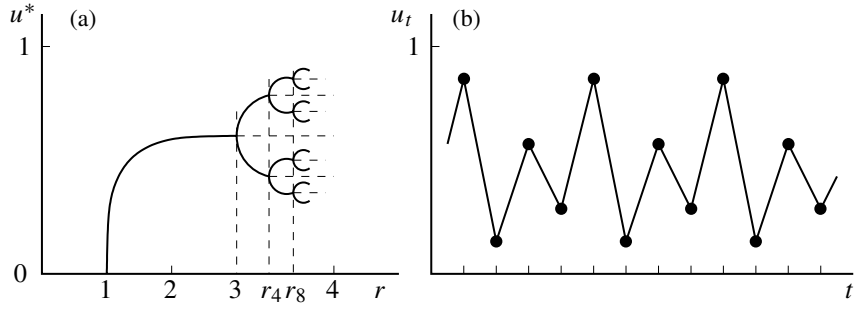

Figure 2.8. (**a**) Stable solutions (schematic) for the logistic model (2.11) as r passes through bifurcation values. At each bifurcation, the previous state becomes unstable and is represented by the dashed lines. The sequence of stable solutions has periods $2, 2^2, 2^3, \ldots$. (**b**) An example (schematic) of a 4-cycle periodic solution where $r_4 < r < r_8$ where r_4 and r_8 are the bifurcation values for 4-period and 8-period solutions respectively.

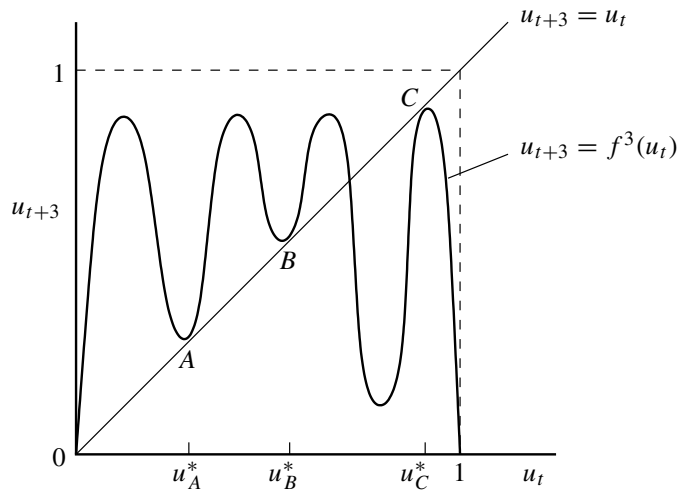

Figure 2.9. Schematic third iterate $u_{t+3} = f^3(u_t)$ for (2.11) at $r = r_c$, the parameter value where the three steady states A, B and C all have eigenvalue $\lambda = 1$. The curve is symmetric about $u_t = 1/2$.

$u_{t+3} = u_t$, that is, the eigenvalue $\lambda = 1$ at these steady states of $u_{t+3} = f^3(u_t)$, we have a 3-cycle. This situation is shown schematically in Figure 2.9. For the model (2.11) the critical $r \approx 3.828$.

Sarkovskii (1964) published an important paper on one-dimensional maps, which has dramatic practical consequences, and is directly related to the situation in Figure 2.9. He proved, among other things, that if a solution of *odd* (≥ 3) period exists for a value r_3 then aperiodic or *chaotic solutions* exist for $r > r_3$. Such solutions simply oscillate in an apparently random manner. The bifurcation here, at r_3, is called a *tangent bifurcation*: the name is suggestive of the situation illustrated in Figure 2.9. Figure 2.10 illustrates some solutions for the model equation (2.4) for various r, including chaotic examples in Figures 2.10(d) and (f). Note the behaviour in Figure 2.10(f), for example: there is population explosion, crashback and slow recovery.

Sarkovskii's theorem was further extended by Stefan(1977). Li and Yorke's (1975) result, namely, that if a period 3 solution exists then solutions of period n exist for all $n \geq 1$, is a special case of Sarkovskii's theorem.

Although we have concentrated here on the logistic model (2.11) this kind of behaviour is typical of difference equation models with the dynamics like (2.1) and schematically illustrated in Figure 2.2; that is, they all exhibit bifurcations to higher periodic solutions eventually leading to chaos.

Figures 2.10(d)–(f) illustrate an interesting aspect of the paths to chaos. As r increases from its value giving the aperiodic solution in Figure 2.10(d) we again get periodic solutions, as in Figure 2.10(e). For larger r, aperiodic solutions again appear as in Figure 2.10(f). So as r increases beyond where chaos first appears there are windows of parameter values where the solution behaviour is periodic. There are thus parameter windows of periodicity interlaced with windows of aperiodicity. Figure 2.11 shows a typical figure obtained when the iterative map is run after a long time, the order of sev-

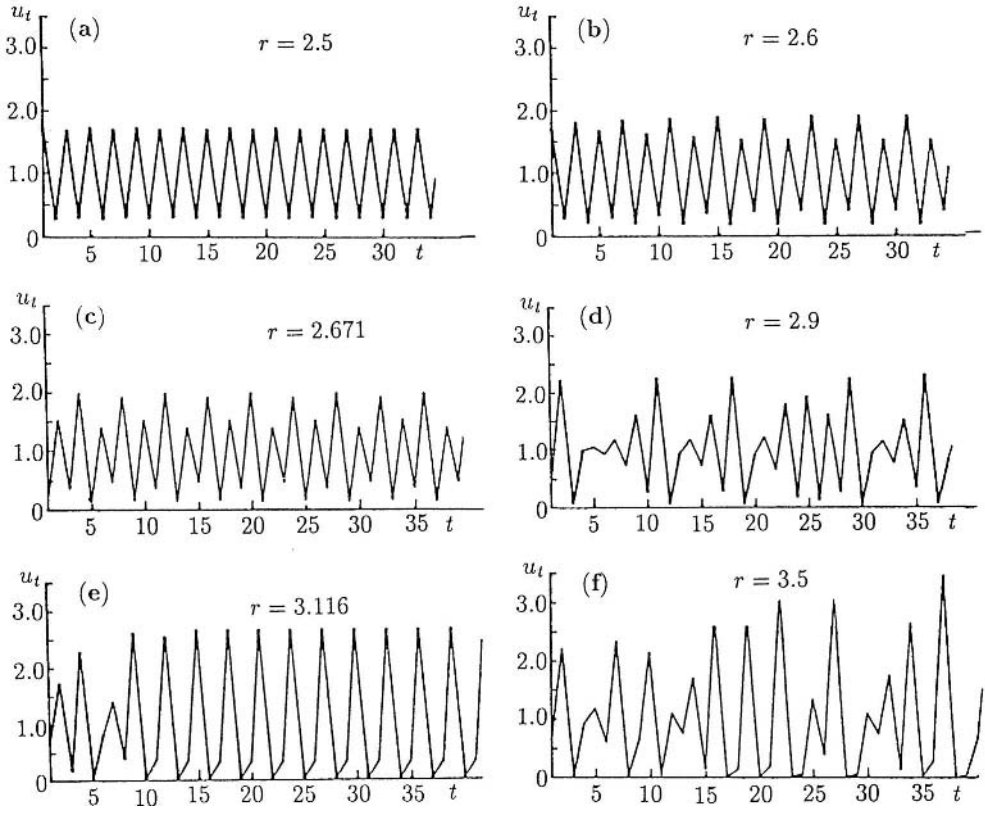

Figure 2.10. Solutions u_t of the model system $u_{t+1} = u_t \exp[r(1 - u_t)]$ for various r. Here the first bifurcation to periodicity occurs at $r = 2$. The larger the parameter r, the larger the amplitude of the oscillatory solution. (**a**), (**b**), and (**c**) exhibit 2-, 4- and 8-cycle periodic solutions, (**d**) and (**f**) chaotic behaviour and (**e**) a 3-cycle solution.

eral thousand iterations, and then run for many more iterations during which the values u_t were plotted.

Refer now to Figure 2.11 and consider the effect on the solutions of increasing r. For $r_2 < r < r_4$ the solution u_t simply oscillates between the two points, A and B, for example, which are the intersections of a vertical line through the r-value. For $r_4 < r < r_8$, u_t exhibits a 4-period solution with the values again given by the intersection of the curves with the vertical line through the r-value as shown. For values of $r_c < r < r_p$ the solutions are chaotic. For a small window of r-values greater than r_p the solutions again exhibit regular periodic solutions after which they are again aperiodic. The sequence of aperiodicity–periodicity–aperiodicity is repeated. If we now look at the inset which is an enlargement of the small rectangle, we see the same sequence of bifurcations repeated in a fractal sense. A brief introduction to fractals is given in Chapter 14, and a short discussion of them in a biological context in Chapter 3, Section 3.9. The elegant book by Peitgen and Richter (1986) shows a colourful selection of spec-

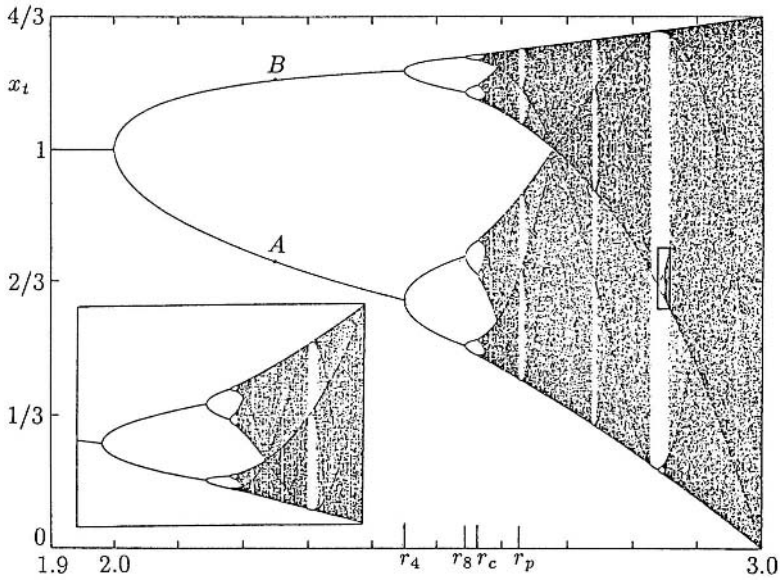

Figure 2.11. Long time asymptotic iterates for the discrete equation $x_{t+1} = x_t + rx_t(1 - x_t)$ for $1.9 < r < 3$. By a suitable rescaling, ($u_t = [r/(r+1)]x_t$, 'r' $= 1 + r$), this can be written in the form (2.11). These are typical of discrete models which exhibit period doubling and eventually chaos and the subsequent path through chaos. Another example is that used in Figure 2.10; see text for a detailed explanation. The enlargement of the small window (with a greater magnification in the r-direction than in the x_t direction) shows the fractal nature of the bifurcation sequences. (Reproduced with permission from Peitgen and Richter 1986; some labelling has been added)

tacular figures and fractal sequences which can arise from discrete models, particularly with two-dimensional models: we discuss a practical application in Chapter 5.

There is increasing interest and a large amount of research going on in chaotic behaviour related to what we have been discussing, much of it prompted by new and potential applications in a variety of different fields. In the popular press it is now referred to as *chaos theory* or the new(!) *nonlinear theory*. (There is nothing like a really immediately recognisable name to get the public's attention; catastrophe theory and fractal theory are others.) The interest is not restricted to discrete models of course: it was first demonstrated by a system of ordinary differential equations—the Lorenz system (Lorenz 1963: see Sparrow 1982, 1986 for a review). This research into chaos has produced many interesting and unexpected results associated with models such as we have been discussing here, namely, those which exhibit periodic doubling. For example, if $r_2, r_4, \ldots r_{2n}, \ldots$ is the sequence of period doubling bifurcation values, Feigenbaum (1978) proved that

$$\lim_{n\to\infty} \frac{r_{2(n+1)} - r_{2n}}{r_{2(n+2)} - r_{2(n+1)}} = \delta = 4.66920\ldots .$$

He showed that δ is a universal constant; that is, it is the value for the equivalent ratio for general iterative maps of the form $u_{t+1} = f(u_t)$, where $f(u_t)$ has a maximum similar to that in Figure 2.2, and which exhibit period doubling.

A useful, practical and quick way to show the existence of chaos has been given by Li et al. (1982). They proved that if, for some u_t and any $f(u_t)$, an *odd* integer n exists such that

$$f^n(u_t; r) < u_t < f(u_t; r)$$

then an *odd* periodic solution exists, which thus implies chaos. For example, with

$$u_{t+1} = f(u_t; r) = u_t \exp[r(1 - u_t)]$$

if $r = 3.0$ and $u_0 = 0.1$, a computation of the first few terms shows

$$u_7 = f^5(u_2) < u_2 < f(u_2) = u_3,$$

that is, $n = 5$ in the above inequality requirement. Hence this $f(u_t; r)$ with $r = 3$ is chaotic.

2.4 Stability, Periodic Solutions and Bifurcations

All relevant population models involve at least one parameter, r say. From the above discussion, as this parameter varies the solutions of the general model equation

$$u_{t+1} = f(u_t; r), \tag{2.17}$$

will usually undergo bifurcations at specific values of r. Such bifurcations can be to periodic solutions with successively higher periods ultimately generating chaotic solutionsfor r greater than some finite critical r_c. From the graphical analysis such bifurcations occur when the appropriate eigenvalues λ pass through $\lambda = 1$ or $\lambda = -1$. Here we discuss some analytical results associated with these bifurcations. For algebraic simplicity we shall often omit the r in $f(u_t; r)$ (unless we want to emphasise a point) by writing $f(u_t)$ but the dependence on a parameter will always be understood. The functions f we have in mind are qualitatively similar to that illustrated in Figure 2.2.

The equilibrium points or fixed points of (2.17) are solutions of

$$u^* = f(u^*; r) \quad \Rightarrow \quad u^*(r). \tag{2.18}$$

To investigate the linear stability of u^* we write, in the usual way,

$$u_t = u^* + v_t, \quad |v_t| \ll 1. \tag{2.19}$$

Substituting this into (2.17) and expanding for small v_t, using a Taylor expansion, we get

$$u^* + v_{t+1} = f(u^* + v_t)$$
$$= f(u^*) + v_t f'(u^*) + O(v_t^2), \mid v_t \mid \ll 1.$$

Since $u^* = f(u^*)$ the linear (in v_t) equation which determines the linear stability of u^* is then

$$v_{t+1} = v_t f'(u^*) = \lambda v_t, \quad \lambda = f'(u^*),$$

where λ is the eigenvalue of the first iterate (2.17) at the fixed point u^*. The solution is

$$v_t = \lambda^t v_0 \to \begin{cases} 0 \\ \pm\infty \end{cases} \quad \text{as} \quad t \to \infty \quad \text{if} \quad \mid \lambda \mid \begin{cases} < 1 \\ > 1 \end{cases}.$$

Thus

$$u^* \quad \text{is} \quad \begin{cases} \text{stable} \\ \text{unstable} \end{cases} \quad \text{if} \quad \begin{cases} -1 < f'(u^*) < 1 \\ \mid f'(u^*) \mid > 1 \end{cases}. \tag{2.20}$$

If u^* is stable, any small perturbation from this equilibrium decays to zero, monotonically if $0 < f'(u^*) < 1$, or with decreasing oscillations if $-1 < f'(u^*) < 0$. On the other hand, if u^* is unstable any perturbation grows monotonically if $f'(u^*) > 1$, or by growing oscillations if $f'(u^*) < -1$. This is all as we deduced before by graphical arguments.

As an example, the rescaled model (2.8) is

$$u_{t+1} = u_t \exp[r(1 - u_t)], \quad r > 0. \tag{2.21}$$

Here the steady states are

$$u^* = 0 \quad \text{or} \quad 1 = \exp[r(1 - u^*)] \quad \Rightarrow \quad u^* = 1. \tag{2.22}$$

Thus the corresponding eigenvalues are

$$\lambda_{u^*=0} = f'(0) = e^r > 1 \quad \text{for} \quad r > 0,$$

so $u^* = 0$ is unstable (monotonically), and

$$\lambda_{u^*=1} = f'(1) = 1 - r. \tag{2.23}$$

Hence $u^* = 1$ is stable for $0 < r < 2$ with oscillatory return to equilibrium if $1 < r < 2$. It is unstable by growing oscillations for $r > 2$. Thus $r = 2$ is the first bifurcation value. On the basis of the above we expect a periodic solution to be the bifurcation from $u^* = 1$ as r passes through the bifurcation value $r = 2$. For $\mid 1 - u_t \mid$ small (2.21) becomes

$$u_{t+1} \approx u_t[1 + r(1 - u_t)]$$

which is exactly the form simulated in Figure 2.11. If we write it in the form

$$U_{t+1} = (1+r)U_t[1-U_t], \quad \text{where} \quad U_t = \frac{ru_t}{1+r},$$

we get the same as the logistic model (2.11) with $r+1$ in place of r. There we saw that a stable periodic solution with period 2 appeared at the first bifurcation. With example (2.21) the next bifurcation, to a 4-periodic solution, occurs at $r = r_4 \approx 2.45$ and a 6-periodic one at $r = r_6 \approx 2.54$ with aperiodic or chaotic behaviour for $r > r_c \approx 2.57$. The successive bifurcation values of r for period doubling again become progressively closer. The sensitivity of the solutions to small variations in $r > 2$ is quite severe in this model: it is in most of them in fact, at least for the equivalent of r beyond the first few bifurcation values.

After t iterations of u_0, $u_t = f^t(u_0)$, using the notation defined in (2.13). A *trajectory* or *orbit* generated by u_0 is the set of points $\{u_0, u_1, u_2, \dots\}$ where

$$u_{i+1} = f(u_i) = f^{i+1}(u_0), \quad i = 0, 1, 2, \dots .$$

We say that a point is periodic of period m or m-periodic if

$$\begin{aligned} f^m(u_0; r) &= u_0 \\ f^i(u_0; r) &\neq u_0 \quad \text{for} \quad i = 1, 2, \dots, m-1 \end{aligned} \tag{2.24}$$

and that u_0, a fixed point of the mapping f^m in (2.24), is a *period-m fixed point* of the mapping f in (2.17). The points $u_0, u_1, \dots, u_{m-1}$ form an m-cycle.

For the stability of a fixed point (solution) we require the eigenvalue; for the equilibrium state u^* it was simply $f'(u^*)$. We now extend this definition to an m-cycle of points $u_0, u_1, \dots, u_{m-1}$. For convenience, introduce

$$F(u; r) = f^m(u; r), \quad G(u; r) = f^{m-1}(u; r).$$

Then the eigenvalue λ_m of the m-cycle is defined as

$$\begin{aligned} \lambda_m &= \left.\frac{\partial f^m(u; r)}{\partial u}\right]_{u=u_i} \qquad i = 0 \text{ or } 1 \text{ or } 2 \text{ or } \dots \ m-1, \\ &= F'(u_i; r) \\ &= f'(G(u_i; r))G'(u_i; r) \\ &= f'(u_{i-1}; r)G'(u_i; r) \\ &= f'(u_{i-1}; r)\left[\frac{\partial f^{m-1}(u_i; r)}{\partial u}\right]_{u=u_i} \end{aligned} \tag{2.25}$$

and so

$$\lambda_m = \prod_{i=0}^{m-1} f'(u_i; r), \tag{2.26}$$

which shows that the form (2.25) is independent of i.

In summary then, a bifurcation occurs at a parameter value r_0 if there is a qualitative change in the dynamics of the solution for $r < r_0$ and $r > r_0$. From the above discussion we now expect it to be from one periodic solution to another with a different period. Also when the sequence of even periods bifurcates to an odd-period solution the Sarkovskii (1964) theorem says that cycles of every integer period exist, which implies chaos. Bifurcations with $\lambda = -1$ are the period-doubling bifurcations while those with $\lambda = 1$ are the tangent bifurcations.

Using one of the several computer packages currently available which carry out algebraic manipulations, it is easy to calculate the eigenvalues λ for each iterate and hence generate the sequence of bifurcation values r using (2.25) or (2.26). There are systematic analytic ways of doing this which are basically extensions of the above; see, for example, Gumowski and Mira (1980). There are also several approximate methods such as that by Hoppensteadt and Hyman (1977). Since we are mentioning books here, that by Strogatz (1994) is an excellent introductory text. You get some idea of the early interest in chaosfrom the collection of reprints, put together by Cvitanović (1984), of some of the frequently quoted papers, and the book of survey articles edited by Holden (1986); in chemistry, the book by Scott (1991) is a good starting point. Chaos can also be used to mask secret messages by superimposing on the message a chaotic mask, the chaos model being available only to the sender and the recipient, who, on receiving the message unmasks the chaos element. Strogatz (1994) discusses this in more detail. These illustrate only very few of the diverse areas in which chaos has been found and studied.

2.5 Discrete Delay Models

All of the discrete models we have so far discussed are based on the assumption that each member of the species at time t contributes to the population at time $t + 1$: this is implied by the general form (2.1), or (2.17) in a scaled version. This is of course the case with most insects but is not so with many other animals where, for example, there is a substantial maturation time to sexual maturity. Thus the population's dynamic model in such cases must include a delay effect: it is, in a sense, like incorporating an age structure. If this delay, to maturity say, is T time-steps, then we are led to study difference delay models of the form

$$u_{t+1} = f(u_t, u_{t-T}). \tag{2.27}$$

In the model for baleen whales, which we discuss below, the delay T is of the order of several years.

To illustrate the problems associated with the linear stability analysis of such models and to acquire a knowledge of what to expect from delay equations we consider the following simple model, which, even so, is of practical interest.

$$u_{t+1} = u_t \exp[r(1 - u_{t-1})], \quad r > 0. \tag{2.28}$$

This is a delay version of (2.21). The equilibrium states are again $u^* = 0$ and $u^* = 1$. The steady state $u^* = 0$ is unstable almost by inspection; a linearisation about $u^* = 0$ immediately shows it.

We linearise about $u^* = 1$ by setting, in the usual way,

$$u_t = 1 + v_t, \quad |\, v_t \,| \ll 1$$

and (2.28) then gives

$$1 + v_{t+1} = (1 + v_t) \exp[-r v_{t-1}] \approx (1 + v_t)(1 - r v_{t-1})$$

and so

$$v_{t+1} - v_t + r v_{t-1} = 0. \tag{2.29}$$

We look for solutions of this difference equation in the form

$$v_t = z^t \quad \Rightarrow \quad z^2 - z + r = 0$$

which gives two values for z, z_1 and z_2, where

$$z_1, z_2 = \frac{1}{2}[1 \pm (1 - 4r)^{1/2}], \quad r < \frac{1}{4}, \quad z_1, z_2 = \rho e^{\pm i\theta}, \quad r > \frac{1}{4} \tag{2.30}$$

with

$$\rho = r^{1/2}, \quad \theta = \tan^{-1}(4r - 1)^{1/2}, \quad r > \frac{1}{4}.$$

The solution of (2.29), for which the *characteristic equation* is the quadratic in z, is then

$$v_t = A z_1^t + B z_2^t, \tag{2.31}$$

where A and B are arbitrary constants.

If $0 < r < 1/4$, z_1 and z_2 are real, $0 < z_1 < 1$, $0 < z_2 < 1$ and so from (2.31), $v_t \to 0$ as $t \to \infty$ and hence $u^* = 1$ is a linearly stable equilibrium state. Furthermore the return to this equilibrium after a small perturbation is monotonic.

If $r > 1/4$, z_1 and z_2 are complex with $z_2 = \overline{z}_1$, the complex conjugate of z_1. Also $z_1 z_2 = |\, z_1 \,|^2 = \rho^2 = r$. Thus for $1/4 < r < 1$, $|\, z_1 \,||\, z_2 \,| < 1$. In this case the solution is

$$v_t = A z_1^t + B \overline{z}_1^t$$

and, since it is real, we must have $B = \overline{A}$ and so, with (2.30), the real solution

$$v_t = 2|\, A \,|\rho^t \cos(t\theta + \gamma), \quad \gamma = \arg A, \quad \theta = \tan^{-1}(4r - 1)^{1/2}. \tag{2.32}$$

As $r \to 1$, $\theta \to \tan^{-1}\sqrt{3} = \pi/3$.

As r passes through the critical $r_c = 1$, $|\, z_1 \,| > 1$ and so v_t grows unboundedly with $t \to \infty$ and u^* is then unstable. Since $\theta \approx \pi/3$ for $r \approx 1$ and $v_t \approx 2|\, A \,| \cos(t\pi/3 + \gamma)$, which has a period of 6, we expect the solution of (2.28), at least for r just greater than

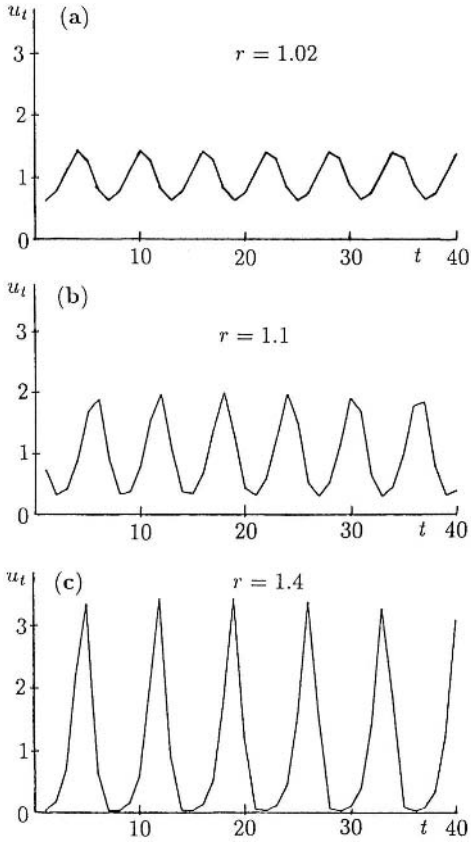

Figure 2.12. Solutions of the delay difference equation (2.28), $u_{t+1} = u_t \exp[r(1 - u_{t-1})]$ for three values of $r > r_c = 1$. (**a**) $r = 1.02$. This shows the 6-period solution which bifurcates off the steady state at $r = r_c$. (**b**) $r = 1.1$. Here, elements of a 6-cycle still exist but these are lost in (**c**), where $r = 1.4$.

$r_c(= 1)$, to exhibit a 6-cycle periodic solution. Figure 2.12 illustrates the computed solution for three values of $r > 1$. In Figure 2.12(b) there are still elements of a 6-cycle, but they are irregular. In Figure 2.12(c) the element of 6-periodicity is lost and the solution becomes more spikelike, often an early indication of chaos.

In the last chapter we saw how delay had a destabilising effect and it increased with increasing delay. It has a similar destabilising effect in discrete models as is clear from comparing the r-values in Figures 2.10 and 2.12. In the former, the critical $r_c = 2$ and the solution bifurcates to a 2-period solution, whereas in the latter delay case the critical $r_c = 1$ and bifurcation is to a 6-period solution. Again, the longer the delay the greater the destabilising effect. This is certainly another reason why the modelling and analysis in the following example gave cause for concern. Higher period solutions are often characterised by large population swings and if the crash-back to low population levels from a previous very high one is sufficiently severe, extinctionis a distinct possibility. Section 2.7 briefly discusses a possible path to extinction.

To conclude this section we briefly describe a practical model used by the International Whaling Commission (IWC) for the baleen whale. The aim of the IWC is to manage the whale population for a sustained yield, prevent extinction, and so on. The

commercial and cultural pressures on the IWC are considerable. To carry out its charter requirements in a realistic way it must understand the dynamics of whale population growth and its ecology.

A model for the now protected baleen whale which the IWC used is based on the discrete-delay model for the population N_t of sexually mature whales at time t,

$$N_{t+1} = (1-\mu)N_t + R(N_{t-T}). \tag{2.33}$$

Here $(1-\mu)N_t$, with $0 < \mu < 1$, is the surviving fraction of whales that contribute to the population a year later and $R(N_{t-T})$ is the number which augments the adult population from births T years earlier. The delay T is the time to sexual maturity and is of the order of 5–10 years. This model assumes that the sex ratio is 1 and the mortality is the same for each sex. The crux of the model is the form of the recruitment term $R(N_{t-T})$ which in the IWC model (see, for example, IWC 1979) is

$$R(N) = \frac{1}{2}(1-\mu)^T N \left\{ P + Q\left[1 - \left(\frac{N}{K}\right)^z\right]\right\}. \tag{2.34}$$

Here K is the unharvested equilibrium density, P is the per capita fecundity of females at $N = K$ with Q the maximum increase in the fecundity possible as the population density falls to low levels, and z is a measure of the severity with which this density is registered. Finally $1-\mu$ is the probability that a newborn whale survives each year and so $(1-\mu)^T$ is the fraction that survives to adulthood after the required T years: the $1/2$ is because half the whales are females and so the fecundity of the females has to be multiplied by $N/2$. This specific model has been studied in detail by Clark (1976a). Further models in fisheries management generally, are discussed by Getz and Haight (1989).

The parameters μ, T and P in (2.33) and (2.34) are not independent. The equilibrium state is

$$N^* = N_{t+1} = N_t = N_{t-T} = K \quad \Rightarrow \quad \mu = \frac{1}{2}(1-\mu)^T P = h \tag{2.35}$$

which, as well as defining h, relates the fecundity P to the mortality μ and the delay T. Independent measurement of these gives a rough consistency check. If we now rescale the model with $u_t = N_t/K$, (2.33), with (2.34), becomes

$$u_{t+1} = (1-\mu)u_t + hu_{t-T}[1 + q(1-u_{t-T}^z)], \tag{2.36}$$

where h is defined in (2.35) and $q = Q/P$. Linearising about the steady state $u^* = 1$ by writing $u_t = 1 + v_t$ the equation for the perturbation is

$$v_{t+1} = (1-\mu)v_t + h(1-qz)v_{t-T}. \tag{2.37}$$

On setting $v_t \propto s^t$,

$$s^{T+1} - (1-\mu)s^T + h(qz-1) = 0, \tag{2.38}$$

which is the characteristic equation. The steady state becomes unstable when $|s| > 1$. Here there are 4 parameters μ, T, h, and qz and the analysis centres around a study of the roots of (2.38); see the paper by Clark (1976b). Although they are complicated, we can determine the conditions on the parameters such that $|s| < 1$ by using the Jury conditions (see Appendix B). The Jury conditions are inequalities that the coefficients of a real polynomial must satisfy for the roots to have modulus less than 1. For polynomials of order greater than about 4, the conditions are prohibitively unwieldy. When $|s| > 1$, as is now to be expected, solutions of (2.33) exhibit bifurcations to periodic solutions with progressively higher periods ultimately leading to chaos; the response parameter z is critical.

Chaos and Data

Chaos is not really a particularly good name for the seemingly random chaotic behaviour exhibited by the solutions of deterministic equations such as we have been discussing. When we look at complex experimental data and seek to model it with a simple model we are implying that the underlying mechanism is actually quite simple. So, when confronting real data it is important to know whether or not the random nature is truly stochastic or chaotic in the deterministic sense here. Not surprisingly this turns out to be a difficult and controversial problem. Although we may have some biological insight as to what the mechanism might be governing the process and generating the data it is unlikely we shall know it with sufficient certainty to be able to write down an exact model for the mechanism. There are several methods which have been developed to try to determine whether or not the data are stochastic or deterministically chaotic but none is foolproof.

To appreciate the difficulty suppose we have data points, N_t say, which measure some population at discrete times, t. If we plot N_t against N_{t+1} and we obtain a relatively smooth curve, say, one qualitatively like that in Figure 2.2, then it would be reasonable to suggest a deterministic model for the generating mechanism, namely, a model such as we have discussed here which can give rise to deterministic chaos. In other words, we are finding a qualitative form for the $f(N_t)$ in (2.1). However, if it does not give any sort of reasonable curve we cannot deduce that the underlying mechanism is not deterministic. For example, in this section we saw that delay can be involved quite naturally in a renewal process. In that case perhaps we could do a three-dimensional plot with N_{t-1} and N_t against N_{t+1}. If a relatively smooth surface results then it could be a deterministic mechanism. Once again if it still gives a random number of points in this space it again does not necessarily point to a nondeterministic model since the relationship between N_t and N_{t+1}, or indeed N_{t-1} or any other population value at earlier times might simply be a more complex discrete model or involve more than one delay. The choices are almost unlimited when seeking to determine the relationship from data.

A sound knowledge of the biology can, of course, considerably reduce the number of possibilities. So, one approach is, for example, to try to determine a plausible model a priori and, if it seems that only N_t and N_{t+1} say, are involved at any time-step then the data can sometimes be used to determine the quantitative details of the functional relationship between the N_t and N_{t+1}. A surprisingly successful example of this arose in the unlikely area of marital interaction and divorce prediction which we discuss in

Chapter 5; see Cook et al. (1995) and the book by Gottman et al. (2002) on a general theory of marriage. Here discrete coupled equations constitute the preliminary model.

A totally different example of how chaotic solutions of discrete equations can give insight into a biological process is given by Cross and Cotton (1994). We discuss the problem and their model and analysis below in Section 2.8.

2.6 Fishery Management Model

Discrete models have been used in fishery management for some considerable time. They have often proven to be useful in evaluating various harvesting strategies with a view to optimising the economic yield and to maintaining it. However, the comments made at the end of Section 1.6 in Chapter 1 should very much be kept in mind. Just a few of the relevant books on management strategies are those by Clark (1976b, 1985, 1990), Goh (1982), Getz and Haight (1989), Hilborn and Mangel (1997), the series of papers edited by Cohen (1987) and appropriate sections in the collection of articles edited by Levin (1994). The following model is applicable, in principle, to any renewable resource which is harvested; the detailed analysis applies to any population whose dynamics can be described by a discrete model.

Suppose that the population density is governed by $N_{t+1} = f(N_t)$ in the absence of harvesting. If we let h_t be the harvest taken from the population at time t, which generates the next population at $t + 1$, then a model for the population dynamics is

$$N_{t+1} = f(N_t) - h_t. \tag{2.39}$$

The questions we address here are: (i) What is the maximum sustained biological yield? (Compare with Section 1.5 in Chapter 1.) (ii) What is the maximum economic yield?

In equilibrium, $N_t = N^* = N_{t+1}$, $h_t = h^*$ where, from (2.39),

$$h^* = f(N^*) - N^*. \tag{2.40}$$

The maximum sustained steady state yield Y_M is when $N^* = N_M$ where

$$\frac{\partial h^*}{\partial N^*} = 0 \quad \Rightarrow \quad f'(N^*) = 1 \quad \text{and} \quad Y_M = f(N_M) - N_M. \tag{2.41}$$

The only situation of interest of course is when $Y_M \geq 0$.

A management strategy could be simply to maintain the population so as to get the maximum yield Y_M. Since it is hard to know what the actual fish population is, this can be difficult to accomplish. What is known is the actual yield and how much effort has gone into getting it. So it is better to formulate the optimization problem in terms of yield and effort.

Let us suppose that a unit effort to catch fish results in a harvest cN from a population N. The constant c is the 'catchability' parameter which is independent of the population density N. Then the effort to reduce N by 1 unit is $1/cN$ and $f(N)$ by 1

unit is $1/(cf(N))$. Thus the effort E_M to provide for a yield

$$Y_M = f(N_M) - N_M \quad \text{is} \quad E_M = \sum_{N_i=N_M}^{f(N_M)} (cN_i)^{-1}.$$

Now if cN is large compared with 1 unit, we can approximate the summation in the last equation by an integral and so

$$E_M \approx \frac{1}{c} \int_{N_M}^{f(N_M)} N^{-1} dN = \frac{1}{c} \ln \left\{ \frac{f(N_M)}{N_M} \right\}. \tag{2.42}$$

The two equations (2.41) and (2.42) give the relation between E_M and Y_M parametrically in N_M.

As an example suppose the unharvested dynamics is governed by $N_{t+1} = f(N_t) = bN_t/(a + N_t)$ with $0 < a < b$; then

$$N_M: \quad 1 = f'(N_M) = \frac{ab}{(a + N_M)^2} \quad \Rightarrow \quad N_M = a^{1/2}(b^{1/2} - a^{1/2}).$$

Substituting this into (2.41) and (2.42) gives

$$Y_M = \frac{bN_M}{(a + N_M)} - N_M, \quad E_M = \frac{1}{c} \ln \left\{ \frac{b}{(a + N_M)} \right\}. \tag{2.43}$$

In this example we can get an explicit relation between Y_M and E_M, on eliminating N_M, as

$$Y_M = [b \exp(-cE_M) - a][\exp(cE_M) - 1]. \tag{2.44}$$

Figure 2.13(a) illustrates the $Y_M - E_M$ relation. Using this, a crucial aspect of a management strategy is to note that if an increase in effort reduces the yield, then the maximum

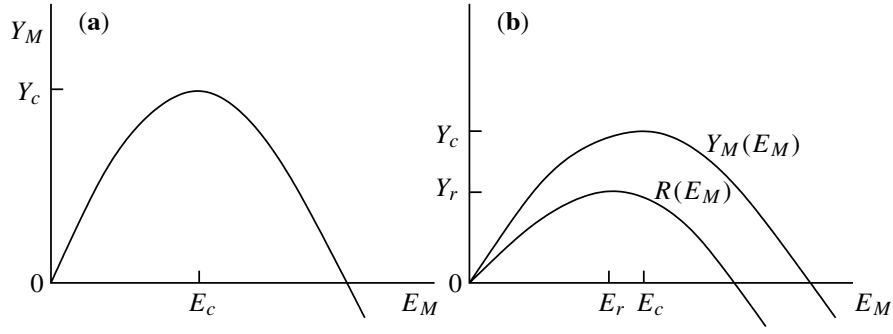

Figure 2.13. (**a**) The yield–effort relation (schematic) for the maximum sustained yield with the model dynamics $N_{t+1} = bN_t/(a + N_t)$, $0 < a < b$. (**b**) The maximum revenue R as a function of the effort E as compared with the $Y_M - E_M$ curve.

sustained yield is exceeded, and the effort has to be reduced so that the population can recover. The effort can subsequently be retuned to try to achieve Y_c with E_c in Figure 2.13(a), both of which can be calculated from (2.44). This analysis is for the maximum sustained biological yield. The maximum economic yield must include the price for the harvest and the cost of the effort. As a first model we can incorporate these in the expression for the economic return $R = pY_M - kE_M$ where p is the price per unit yield and k is the cost per unit effort. Using (2.43) for $Y_M(N_M)$ and $E_M(N_M)$ we thus have $R(N_M)$ which we must now maximise. We thus get a curve for the maximum revenue R as a function of the effort E; it is illustrated in Figure 2.13(b).

Such 'model' results must not be taken too seriously unless backed up by experimental observation. They can, however, give some important qualitative pointers. Our analysis here has been based on the fact that the harvested population has a steady state. Fish, in particular, have a high per capita growth rate which, in the detailed models we have analysed, is related to the parameter r. We would expect, therefore, that the fish population would exhibit periodic fluctuations and this is known to be the case. It is possible that the growth rate is sufficiently high that the behaviour may, in some cases, be in the chaotic regime. Since harvesting is, in a sense, an effective lowering of the reproduction rate it is feasible that it could have a stabilising effect, for example, from the chaotic to the periodic or even to a steady state situation.

2.7 Ecological Implications and Caveats

A major reason for modelling the dynamics of a population is to understand the principle controlling features and to be able to predict the likely pattern of development consequent upon a change of environmental parameters. In making the model we may have, to varying degrees, a biological knowledge of the species and observational data with which to compare the results of the analysis of the model. It may be helpful to summarise what we can learn about a population's dynamics from the type of models we have considered and to point out a few of their difficulties and limitations.

When a plausible model for a population's growth dynamics has been arrived at, the global dynamics can be determined. Using graphical methods the changes in the solutions as a major environment parameter varies can also be seen. From Figure 2.4, for example, we see that if we start with a low population, it simply grows for a while, then it can appear to oscillate quasi-regularly and then settle down to a constant state, or exhibit periodic behaviour or just oscillate in a seemingly random way with large populations at one stage and crash to very low densities in the following time-step. Whatever the model, as long as it has a general form such as in Figure 2.6 the population density is always bounded.

This seemingly random dynamics poses serious problems from a modelling point of view. Are the data obtained which exhibit this kind of behaviour generated by a deterministic model or by a stochastic situation? It is thus a problem to decide which is appropriate and it may not actually be one we can resolve in a specific situation. What modelling can do, however, is to point to how sensitive the population dynamics can be to changes in environmental parameters, the estimation of which is often difficult and usually important.

The type of dynamics exhibited with $f(N_t)$ such as in Figure 2.6, shows that the population is always bounded after a long time by some maximum $N_{\max}$ and minimum $N_{\min}$: the first few iterations can lie below $N_{\min}$ if N_0 is sufficiently small. With Figure 2.6 in mind the maximum $N_{\max}$ is given by the first iteration of the value where $N_{t+1} = f(N_t)$ has a maximum, N_m say. That is,

$$\frac{df}{dN_t} = 0 \quad \Rightarrow \quad N_m, \quad N_{\max} = f(N_m).$$

The minimum $N_{\min}$ is then the first iterative of $N_{\max}$, namely,

$$N_{\min} = f(N_{\max}) = f(f(N_m)) = f^2(N_m). \tag{2.45}$$

These ultimately limiting population sizes are easy to work out for a given model. For example, with

$$\begin{aligned} &N_{t+1} = f(N_t) = N_t \exp\left[r\left(1 - \frac{N_t}{K}\right)\right], \quad f'(N_t) = 0 \quad \Rightarrow \quad N_m = \frac{K}{r} \\ &N_{\max} = f(N_m) = \frac{K}{r} e^{r-1}, \\ &N_{\min} = f(f(N_m)) = \frac{K}{r} \exp\left[2r - 1 - e^{r-1}\right]. \end{aligned} \tag{2.46}$$

With a steeply decreasing behaviour of the dynamics curve $N_{t+1} = f(N_t)$ for $N_t > N_m$, the possibility of a dramatic drop in the population to low values close to $N_{\min}$ brings up the question of *extinction* of a species. If the population drops to a value $N_t < 1$ the species is clearly extinct. In fact extinction is almost inevitable if N_t drops to low values. At this stage a stochastic model is required. However an estimate of when the population drops to 1 or less, and hence extinction, can be obtained from the evaluation of $N_{\min}$ for a given model. The condition is, using (2.45),

$$N_{\min} = f^2(N_m) \leq 1, \quad \left.\frac{df}{dN}\right|_{N=N_m} = 0. \tag{2.47}$$

With the example in (2.46) this condition is

$$\frac{K}{r} \exp\left[2r - 1 - e^{r-1}\right] \leq 1.$$

So if $r = 3.5$ say, and if $K < 1600$ approximately, the population will eventually become extinct.

An important phenomenon is indicated by the analysis of this model (2.46); the larger the reproduction parameter r the smaller is $N_{\min}$ and the more likelihood of a population crash which will make the species extinct. Note also that it will usually be the case that the population size immediately before the catastrophic drop is large. With the above example if $r = 3.5$ it is almost 3500, from (2.46). An interesting and

potentially practical application of the concept of extinctionis that of introducing sterile species of a pest to try to control the numbers; see Exercise 6 below. The high cost of such a procedure, however, is often prohibitive.

An important group of models not specifically discussed up to now but which come into the general class (2.1) is those which exhibit the *Allee effect*. Biological populations which show this effect decrease in size if the population falls below a certain threshold level N_c say. A typical density-dependent population model which illustrates this is shown in Figure 2.14. If we start with a population, N_0 say, such that $f^2(N_0) < N_c$ then $N_t \to 0$. Such models usually arise as a result of predation. The continuous time model for the budworm equation (1.6) in Chapter 1, has such a behaviour. The region $N_t < N_c$ is sometimes called the *predation pit*. Here $N_t = 0, N_c, N^*$ are all steady states with $N_t = 0$ stable, N_c unstable and N^* stable or unstable depending on $f'(N^*)$ in the usual way. With this type of dynamics, extinction is inevitable if $N_t < N_c$, irrespective of how large N_c may be. Models which show an Allee effect display an even richer spectrum of behaviour than those we considered above, namely, all of the exotic oscillatory behaviour plus the possibility of extinction if any iterate $f^m(N_t) < N_c$ for some m.

The implications from nonlinear discrete models such as we have considered in this chapter rely crucially on the biological parameters obtained from an analysis of observational data. Southwood (1981) discussed, among other things, these population parameters and presented hard facts about several species. Hassell et al. (1976) have analysed a large number of species life data and fitted them to the model $N_{t+1} = f(N_t) = rN_t/(1 + aN_t)^b$ with r, a and b positive parameters; see also the book by Kot (2001). With $b > 1$ this $f(N_t)$ has one hump like those in Figure 2.2. For example, the Colorado beetle is well within the stable periodic regime while Nicholson's (1954) blowflies could be in the chaotic regime.

Finally, it should be emphasised here that the richness of solution behaviour is a result of the nonlinearity of these models. It is also interesting that many of the qualita-

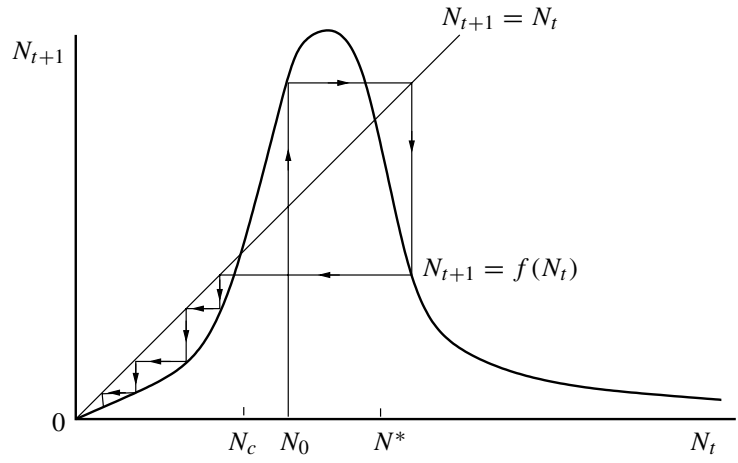

Figure 2.14. A population model which exhibits the Allee effect, whereby if the population $N_t < N_c$ at any time t then $N_t \to 0$, that is, extinction.

tive features can be found by remarkably elementary methods even though they present some sophisticated and challenging mathematical problems.

2.8 Tumour Cell Growth

Cross and Cotton (1994) discuss a problem in pathology, in which the data are given for a population, denoted by N_t, consisting of tumour cells. In their analysis they chose the simple logistic form given by (2.5) with $K = 1$, namely,

$$N_{t+1} = rN_t(1 - N_t), \tag{2.48}$$

where r reflects the growth rate of the tumour cells. The normalisation of N_t to 1 means that N_t is the fraction of the total population of cells that can be sustained in the cell culture container. We know from the analysis in Sections 2.2 through 2.4 that for $r < 3$ the population N_t simply increases until it reaches its steady state $(r - 1)/r$, which it does relatively quickly if N_0 is not too small: for example, if $N_0 = 0.001$ and $r = 2$ the population roughly doubles with each time-step. For $r > 3$ periodic solutions appear, eventually giving rise to chaos for $r > r_c$. With r in the chaotic regime the population of cells at any time, t, would depend critically on the initial conditions. Figure 2.15 illustrates typical population growth for different values of r. In Figure 2.15(b) N_t approaches a periodic solution but in the early stages also exhibits a quasi-sigmoidal growth curve. In Figure 2.15(c) the solution is chaotic.

Suppose multi-clonality is included in the model with the various cell clones having different initial populations. Let us further suppose that their growth rates are different but all with an $r > r_c$ and so they all exhibit chaotic behaviour. A major pathological interest is in the total size of the tumour, that is, the total number of cells. Cross and Cotton (1994) considered first 5 clones and summed their populations to obtain the total population. A typical result is illustrated in Figure 2.16(a). We begin to see the beginning of a smoothing of the chaotic behaviour and the tentative appearance of the sigmoidlike character of the population in Figure 2.15(a). When they included 200 clones the smoothing effect was much more pronounced as illustrated in Figure 2.16(b). Multi-clonality is common in tumour growth and data exhibit growth patterns such as in Figure 2.16(b). With this simple example it is clear that multi-clonality could obscure an underlying deterministic chaos. There are gross assumptions in this model such as assuming that the growth parameter r is constant for each clone for all time. Modelling how cell division varies with time is an interesting problem in its own right because of the transition from discrete division to essential continuous division for an initial group of new cells. It was discussed by Murray and Frenzen (1986). A varying growth parameter in the multi-clone situation suggests that an age-structured model might be more appropriate. It would be interesting to investigate the growth characteristics of a multi-clone system with age structure with each clone in the chaotic growth regime and how variable growth rates and age structure could manifest themselves in experimental observations.

Many biological processes are chaotic, or if not strictly chaotic in the sense here, at the least stochastic, but nevertheless when seen in neurology, pathology and physiology,

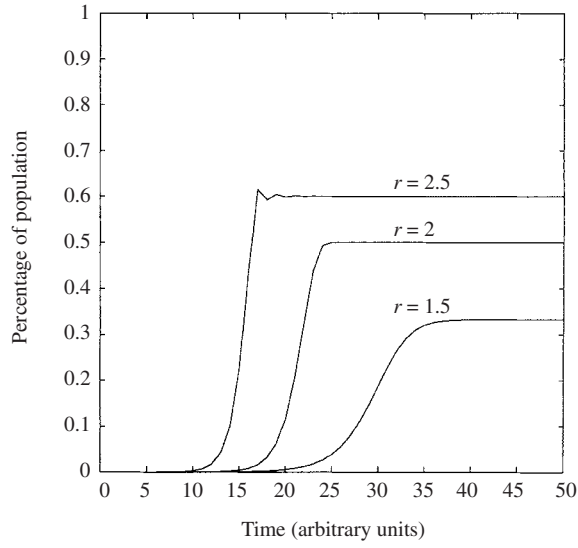

(a)

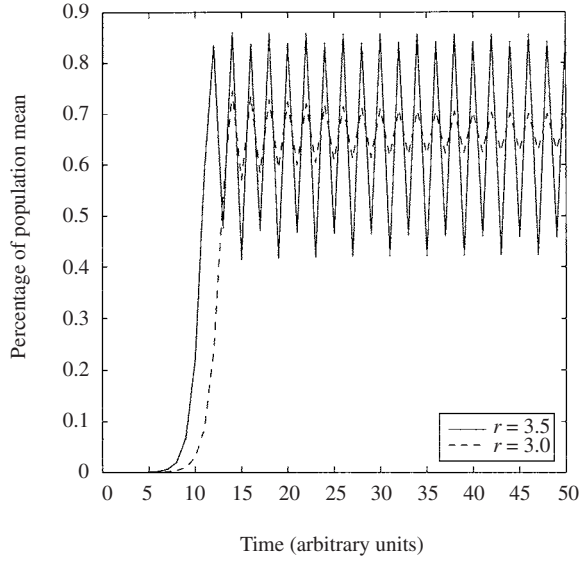

(b)

Figure 2.15. Starting with the same initial populations the graphs display typical cell growth curves—sigmoidal growth curves for various r: (**a**) $0 < r < 3$, (**b**) $3 < r < r_c$. For $r > r_c$ we get typical chaotic behaviour (see also Figure 2.16). Initial value: $N_0 = 10^{-6}$.

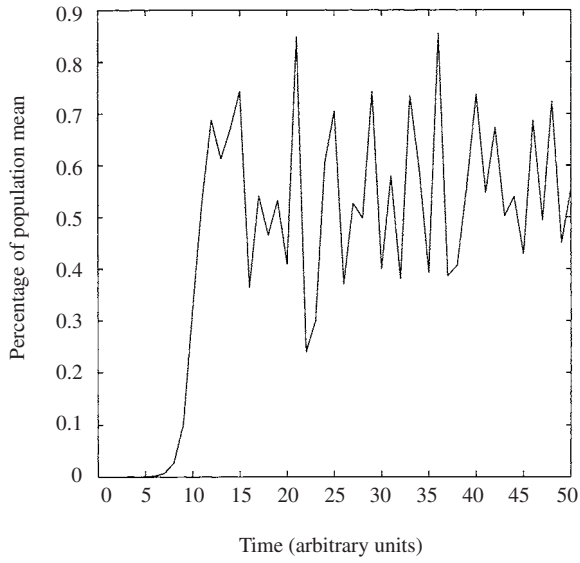

(a)

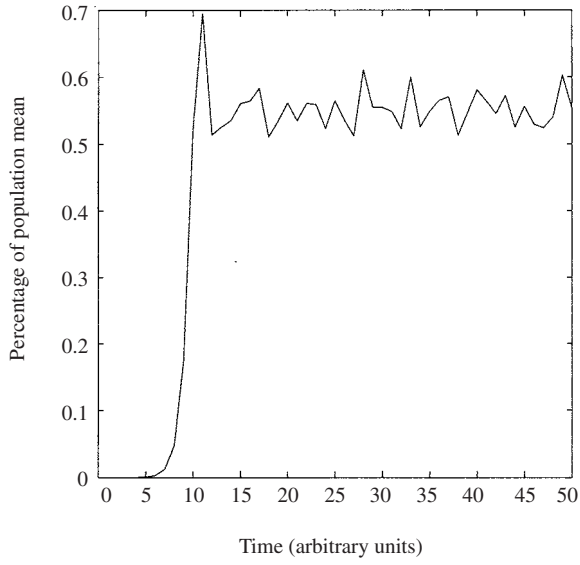

(b)

Figure 2.16. Total mean population fraction N_t with (**a**) 5 clones and (**b**) 200 clones; $r = 3.98$ ($> r_c$). The chaotic smoothing is greater the larger the number of clones, each of which individually exhibits deterministic chaos. The initial conditions were $N_0 = 10^{-6}$ times a random number. (These curves are equivalent to those in Cross and Cotton 1994.)

for example, seem to exhibit considerable order. A recent review of the possible connection with epilepsy is given by Iasemidis and Sackellares (1996). Among other things, one reason they feel it is of relevance is that in many chaotic sytems there are sharply intermittent transitions between regions of chaos—highly disordered states—and highly ordered regions; Figure 2.11 is a typical example. They hypothesize that epilepsy may be an example of chaos and the careful analysis of electroencephalograms with this in mind has provided some new insights into the whole epileptogenetic process. They feel it could have possible use in both the diagnosis and treatment of epilepsy.

An interesting study (Larter et al. 1999) on the role of chaos in brain activity also suggests that chaos is the norm but during an epileptic seizure the activity becomes abnormally regular. In epileptic fits called partial seizures (patients with these are least responsive to medication) only part of the brain starts to exhibit regularity and this spreads and the seizure spreads accordingly. They studied a thousand interconnecting neurons and subjected the equation system to perturbations to try to understand how communication takes place. Among other things they were interested in what affects the rate of transfer from regular behaviour in one region to a neighbouring chaotic region. Their aim also is to apply the results in treating patients who suffer from partial seizures.

In the case of wave activity in the heart (see Chapter 1, Volume II) it is quite the opposite. If regular activity becomes chaotic, a disorder called cardiac fibrillation, it is fatal unless the heart can be shocked back into regularity: the usual method is by a massive electric shock.

Another example, mentioned by Cross and Cotton (1994), is that the growth of human hair is normally asynchronous but there are circumstances when it is synchronised by various (usually disease) stimuli. A common example is during pregnancy and delivery when all the hairs are synchronised in the telogen stage, that is, the resting stage in the cell cycle, the consequence of which is temporary baldness; the condition is called telogen effluvium (Benedict et al. 1991). From the graphs in Figure 2.16 there is increasing order with the number of clones which suggests there is a mechanism for 'antichaos,' a word that is increasingly appearing in the literature. It has similarities to synchronisation which occurs in a variety of biological situations. One example is with certain cells in culture which initially had different cell cycles but can be induced, with an appropriate stimulus, to become synchronised. Another is the synchronisation of fireflies which we discuss later in Chapter 9 where we discuss biological oscillators. A very different type of antichaos has been found by Benchetrit et al. (1987) and Demongeot et al. (1987 and 1996) in the analysis of chaotic breathing patterns. The latter used the concepts of the new field of variability theory, developed by Aubin (1991), and showed how a certain coherent order could be extracted from underlying chaos (in the sense of this chapter). An interesting approach to the concept of attractors and confiners was developed by Demongeot and Jacob (1989) and Cosnard and Demongeot (1985).

Exercises

1 All the following discrete time population models are of the form $N_{t+1} = f(N_t)$ and have been taken from the ecological literature and all have been used in modelling real situations. Determine the nonnegative steady states, discuss their linear stabil-

ity and find the first bifurcation values of the parameters, which are all taken to be positive.

$$\begin{aligned}
&\text{(i)} \quad N_{t+1} = N_t\left[1 + r\left(1 - \frac{N_t}{K}\right)\right],\\
&\text{(ii)} \quad N_{t+1} = rN_t^{1-b}, \quad \text{if} \quad N_t > K,\\
&\qquad\qquad = rN_t, \quad \text{if} \quad N_t < K,\\
&\text{(iii)} \quad N_{t+1} = \frac{rN_t}{(1 + aN_t)^b},\\
&\text{(iv)} \quad N_{t+1} = \frac{rN_t}{1 + \left(\frac{N_t}{K}\right)^b}.
\end{aligned}$$

2 Construct cobweb maps for:

$$\begin{aligned}
&\text{(i)} \quad N_{t+1} = \frac{(1 + r)N_t}{1 + rN_t},\\
&\text{(ii)} \quad N_{t+1} = \frac{rN_t}{(1 + aN_t)^b}, \quad a > 0, \quad b > 0, \quad r > 0
\end{aligned}$$

and discuss the global qualitative behaviour of the solutions. Determine, where possible, the maximum and minimum N_t, and the minimum for (ii) when $b \ll 1$.

3 Verify that an exact solution exists for the logistic difference equation

$$u_{t+1} = ru_t(1 - u_t), \quad r > 0$$

in the form $u_t = A\sin^2\alpha^t$ by determining values for r, A and α. Is the solution (i) periodic? (ii) oscillatory? Describe it! If $r > 4$ discuss possible solution implications.

4 The population dynamics of a species is governed by the discrete model

$$N_{t+1} = f(N_t) = N_t \exp\left[r\left(1 - \frac{N_t}{K}\right)\right],$$

where r and K are positive constants. Determine the steady states and their corresponding eigenvalues. Show that a period-doubling bifurcation occurs at $r = 2$. Briefly describe qualitatively the dynamic behaviour of the population for $r = 2 + \varepsilon$, where $0 < \varepsilon \ll 1$. In the case $r > 1$ sketch $N_{t+1} = f(N_t)$ and show graphically or otherwise that, for t large, the maximum population is given by $N_m = f(K/r)$ and the minimum possible population by $N_m = f(f(K/r))$. Since a species becomes extinct if $N_t \leq 1$ for any $t > 1$, show that irrespective of the size of $r > 1$ the species could become extinct if the carrying capacity $K < r\exp[1 + e^{r-1} - 2r]$.

5 The population of a certain species subjected to a specific kind of predation is modelled by the difference equation

$$u_{t+1} = a\frac{u_t^2}{b^2 + u_t^2}, \quad a > 0.$$

Determine the equilibria and show that if $a^2 > 4b^2$ it is possible for the population to be driven to extinction if it becomes less than a critical size which you should find.

6 It has been suggested that a means of controlling insect numbers is to introduce and maintain a number of sterile insects in the population. One such model for the resulting population dynamics is

$$N_{t+1} = \frac{RN_t^2}{(R-1)\frac{N_t^2}{M} + N_t + S},$$

where $R > 1$ and $M > 0$ are constant parameters, and S is the constant sterile insect population.

Determine the steady states and discuss their linear stability, noting whether any type of bifurcation is possible. Find the critical value S_c of the sterile population in terms of R and M so that if $S > S_c$ the insect population is eradicated. Construct a cobweb map and draw a graph of S against the steady state population density, and hence determine the possible solution behaviour if $0 < S < S_c$.

7 A discrete model for a population N_t consists of

$$N_{t+1} = \frac{rN_t}{1 + bN_t^2} = f(N_t),$$

where t is the discrete time and r and b are positive parameters. What do r and b represent in this model? Show, with the help of a cobweb, that after a long time the population N_t is bounded by

$$N_{\min} = \frac{2r^2}{(4 + r^2)\sqrt{b}} \leq N_t \leq \frac{r}{2\sqrt{b}}.$$

Prove that, for any r, the population will become extinct if $b > 4$.

Determine the steady states and their eigenvalues and hence show that $r = 1$ is a bifurcation value. Show that, for any finite r, oscillatory solutions for N_t are not possible.

Consider a delay version of the model given by

$$N_{t+1} = \frac{rN_t}{1 + bN_{t-1}^2} = f(N_t), \quad r > 1.$$

Investigate the linear stability about the positive steady state N^* by setting $N_t = N^* + n_t$. Show that n_t satisfies

$$n_{t+1} - n_t + 2(r-1)r^{-1}n_{t-1} = 0.$$

Hence show that $r = 2$ is a bifurcation value and that as $r \to 2$ the steady state bifurcates to a periodic solution of period 6.

8 A basic delay model used by the International Whaling Commission (IWC) for monitoring whale populations is

$$u_{t+1} = su_t + R(u_{t-T}), \quad 0 < s < 0,$$

where $T \geq 1$ is an integer.

(i) If u^* is a positive equilibrium show that a sufficient condition for linear stability is $| R'(u^*) | < 1 - s$. [Hint: Use Rouché's theorem on the resulting characteristic polynomial for small perturbations about u^*.]

(ii) If $R(u) = (1 - s)u[1 + q(1 - u)]$, $q > 0$ and the delay $T = 1$, show that the equilibrium state is stable for all $0 < q < 2$. [With this model, T is the time from birth to sexual maturity, s is a survival parameter and $R(u_{t-T})$ the recruitment to the adult population from those born T years ago.]

9 Consider the effect of regularly harvesting the population of a species for which the model equation is

$$u_{t+1} = \frac{bu_t^2}{1 + u_t^2} - Eu_t = f(u_t; E), \quad b > 2, \quad E > 0,$$

where E is a measure of the effort expended in obtaining the harvest, Eu_t. [This model with $E = 0$ is a special case of that in Exercise 5.] Determine the steady states and hence show that if the effort $E > E_m = (b-2)/2$, no harvest is obtained. If $E < E_m$ show, by cobwebbing $u_{t+1} = f(u_t; E)$ or otherwise, that the model is realistic only if the population u_t always lies between two positive values which you should determine analytically.

With $E < E_m$ evaluate the eigenvalue of the largest positive steady state. Demonstrate that a tangent bifurcation exists as $E \to E_m$.